Distribution of Charge in Th^{232} and U^{238} Determined by Measurements on Muonic X Rays

R. E. Coté* and W. V. Prestwich†
Argonne National Laboratory, Argonne, Illinois‡
and
A. K. Gaigalas and S. Raboy
State University of New York at Binghamton, Binghamton, New York 13901§
and
C. C. Trail
Brooklyn College, The City University of New York, Brooklyn, New York
and
R. A. Carrigan, Jr., P. D. Gupta, R. B. Sutton, M. N. Suzuki, and A. C. Thompson
Carnegie-Mellon University, Pittsburgh, Pennsylvania‡

(Received 31 July 1968)

The energies and intensities of the x rays of muonic atoms of Th^{232} and U^{238} were measured. Analysis of the data was performed using the rotational model of strongly deformed nuclei to include dynamic quadrupole interactions. The distribution of nuclear charge was represented by a modified Fermi distribution which involves three parameters, namely, the intrinsic quadrupole moment Q_0, the half-density radius $c=c_0A^{1/3}$, and the skin thickness t. It was found that the allowed ranges of values for Q_0, c_0, and t were for thorium 9.58–9.83 b, 1.155–1.143 F, and 1.54–1.87 F, and for uranium 11.20–11.41 b, 1.150–1.142 F, and 1.600–1.87 F, respectively. However, if specific values for two of these parameters are chosen, the third is determined with an error smaller than the above ranges: 0.5% for Q_0, 0.25% for c_0, and 0.6% for t.

INTRODUCTION

In the pioneering papers of Wilets[1] and Jacobsohn[2] it was pointed out that measurements of the energies of the hyperfine components of the x rays of muonic atoms of deformed even-even nuclei would lead to information about the sign and magnitude of the intrinsic quadrupole moments of these nuclei. With the resolution available in Li-drifted Ge detectors, it is now possible to obtain data sufficiently precise to yield information about the shape as well as the radial distribution of the electric charge in nuclei.

In this paper we report on experiments on muonic x rays of Th^{232} and U^{238}. The analysis of the experimental data follows the suggestions of Wilets and Jacobsohn. That is, we invoke the rotational model of the nucleus for these nuclei, and describe the intrinsic charge distribution by a modified Fermi function with three parameters.

To fit the data, it was necessary to include static and dynamic quadrupole interaction between the nucleus and the muon in the $2p$ and $3d$ states.

EXPERIMENTAL PROCEDURE

The experiment was performed at the synchrocyclotron of Carnegie-Mellon University. A beam of muons extracted through the muon channel was incident on a suitable target as shown in the experimental arrangement of Fig. 1. An x ray associated with the absorption of a muon in the target was identified by a coincidence between pulses from the x-ray crystal detector and pulses from counters 1, 2, 3, in anticoincidence with pulses from counters 4 and the Čerenkov counter.

An absorber of carbon was inserted in the beam to remove the pion contamination. Erroneous events caused by electron contamination were vetoed by the Čerenkov counter. Counter 4 was used to reject events caused by charged particles coming from the target and entering the Ge crystal.

The targets used were about 9 g/cm² thick and about 15 cm×15 cm in area. We were able to obtain a stopping rate in the target of about 10 000 muon/sec. The various crystal detectors used throughout the experiment were provided by H. Mann and his group at Argonne National Laboratory.

The electrical pulses from the crystal detector, when certified by the counters of the muon telescope to be associated with stopping muons, were processed in a SCIPP multichannel analyzer. The data for Th^{232} were collected in an analyzer of 1600 channels, that for U^{238} in 3200 channels.

The counting rate in the Ge(Li) crystal was maintained at the same level for calibration runs and data runs. The radioactive sources used for calibration were kept in the same position for the entire experiment. Appropriate electronic arrangements were made to record the calibration γ rays during the calibration runs which preceded and followed the x-ray runs of about 10 h each. The data reported here are the composite of several such x-ray runs. The thorium sample provided enough γ rays to calibrate the region below 3 MeV. For

* Deceased.
† Present address: McMaster University, Hamilton, Ontario, Canada.
‡ Work supported by U.S. Atomic Energy Commission.
§ Work supported by National Science Foundation under Grant GP6213.
[1] L. Wilets, Kgl. Danske Videnskab Selskab, Mat.-Fys. Medd. 29, No. 3 (1954).
[2] B. A. Jacobsohn, Phys. Rev. 96, 1637 (1954).

calibration in the 6 MeV region, the de-excitation γ ray from O^{16*} was used. This was obtained from the decay $N^{16} \rightarrow O^{16*} + e^- + \bar{\nu}$, the N^{16} being produced through the n-p reaction on oxygen in water flowing past the cyclotron window. During the experiment on U^{238} we kept the Th^{232} sample near the target of U^{238} for calibration purposes. The energies[3,4] of the γ rays used for calibration are given in Table I.

The analyzing system was digitally stabilized by setting a Stirrup Stabilizer on the full energy peak of the γ ray of 2614.47 keV from a Th^{232} source. By stabilizing on only one γ ray we risked possibilities of baseline shifts. The intensity of some of the calibration γ rays were great enough, however, to give us a number of accidental coincidences during the data runs to allow us to obtain calibration peaks while the runs were in progress. It was the comparison of the positions of these accidental feedthroughs with the positions of the calibration lines obtained during the calibration run, which indicates that a small baseline shift in the system was present. This amounted to a shift of about 1.02 ± 0.09 channels for the experiment on U^{238} and 0.29 ± 0.06 channels for the measurements on Th^{232} at the channel position corresponding to 511 keV, for both elements. These shifts are equivalent to shifts of 1.8 and 1.1 keV, respectively. We used the peaks of the calibration lines in accidental coincidence for calibration purposes whenever possible.

The linearity of the system was checked with the γ rays of Ga^{66} and N^{16}. It was established from this check that for regions of about 300 channels, the system was linear to about 0.14%. Therefore, for the determination of the energy of an x ray, we used calibration γ rays which were confined to an energy region of about 300 channels about the x ray of interest.

The positions of the selected peaks of the calibration γ rays and of the x rays were determined by adapting

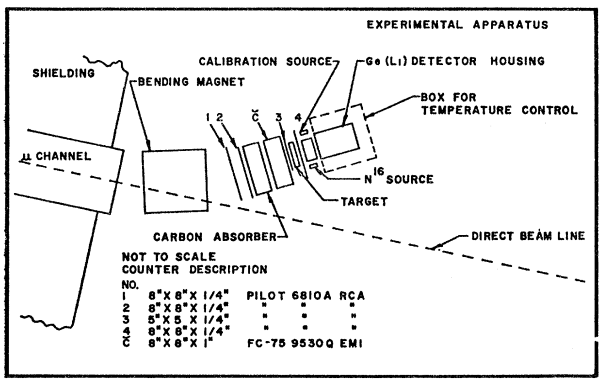

FIG. 1. Schematic drawing of the experimental arrangement.

[3] G. Murray, R. L. Graham, and J. S. Geiger, Nucl. Phys. **63**, 353 (1965).

[4] This value was obtained by averaging results given by C. Chasman, K. W. Jones, R. A. Ristinen, and D. W. Alburger, Phys. Rev. **159**, 830 (1963); R. C. Greenwood, Phys. Letters **23**, 482 (1966); and H. Anderson (private communication).

TABLE I. Values of physical constants used in the calculation.

Rest mass of the muon	$(\mu_0) = 105.659$ MeV
Velocity of light	$(c) = 2.997925 \times 10^{10}$ cm/sec
Fine structure constant	$(\alpha) = 1/137.0388$
Planck's constant	$(h) = 6.5820 \times 10^{-22}$ MeV sec
Mass of the electron	$(m_e) = 0.511006$ MeV
One atomic mass unit	(1 amu) = 931.478 MeV
Mass excess for Th^{232}	0.038211 amu
Mass excess for U^{238}	0.050760 amu

Spins and energies of nuclear levels used

U^{238}	Spin	Energy (keV)
	0	0
	2	44.7
	4	148.0
	6	309.0
Th^{232}	0	0
	2	48.4
	4	155.0

Energies of γ rays used for calibration (keV)	Source
511.006	
583.139 ± 0.023[a]	Bi^{208}
2614.47 ± 0.10[a]	Bi^{208}
6129.58 ± 0.5[b]	N^{16}

[a] Reference 3.
[b] Reference 4.

computational techniques developed at Argonne National Laboratory.[5] The peaks were assumed to be Gaussian in shape, and the parameters of the Gaussian curve were determined by a minimization of the $(\chi)^2$ of the data for this assumed shape.

The experimental data for the K x rays of muonic atoms of Th^{232} and U^{238} are shown in Figs. 2 and 3, respectively. The vertical lines represent a calculated spectrum with the height proportional to the intensity of the transition. The horizontal lines between the transitions indicate pairs of transitions originating from the same $2p$ component but terminating on $1s$ levels corresponding to different nuclear states. Some of the peaks in these spectra are clearly of multiple structure. The theoretically calculated spectra, at the bottom of the figures, was used to predict the number of components in each peak. The location and the amplitude of these peaks were then adjusted to give the minimum χ^2 for the composite spectrum. In the case of the data for U^{238}, the widths of the peaks were one of the param-

[5] R. T. Julke, J. E. Monahan, S. Raboy, and C. C. Trail, Argonne National Laboratory Report No. 6499, 1962 (unpublished).

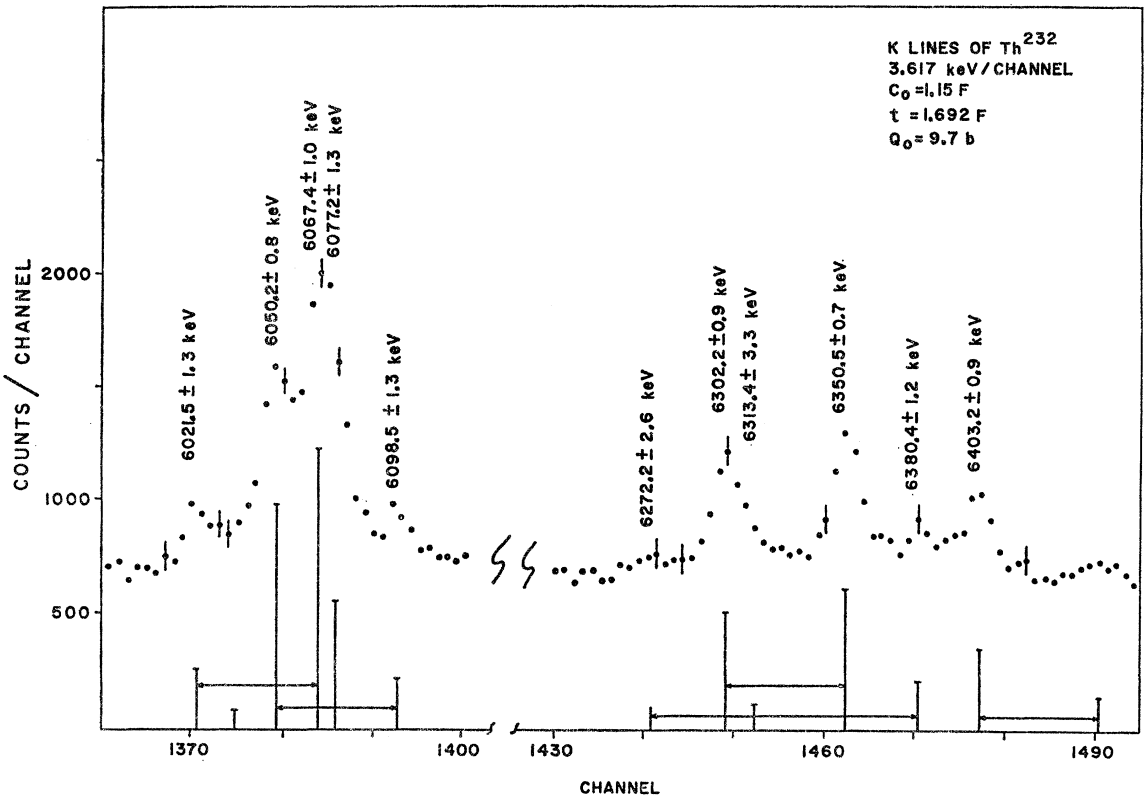

FIG. 2. Spectrum of K x rays (of muonic atoms) of Th^{232}. Vertical lines represent a calculated spectrum for the parameters listed above. The height of the vertical lines is proportional to the intensity. The horizontal lines between certain pairs of vertical lines indicate transitions which differ by the energies of nuclear states.

eters whose value was determined by the computational procedure. The widths were consistent with those expected from calibration linewidths. This technique was unsuccessful for the peaks at the lower energy end of the data for Th^{232}. Our program was revised to prescribe the width, obtained from the calibration standards, as fixed input data.

In Figs. 4–6, we present the data for the L and M x rays. The calibration for the determination of the M and N x rays of muonic atoms of Th^{232} was provided by the peaks caused by accidental coincidences between the pulses from calibration γ rays and the events signifying the absorption of a muon in the target.

The energies of the M and N x rays of U^{238} were corrected for systematic error attributed to shift of the base level in the linear gate of the analyzer. The corrections amounted to 1.8 keV for the N x ray, and 0.6 keV for the M x ray. The statistical errors were increased to take into account the error attributed to the estimate of the baseline shift.

Corrections for the shift of the baseline are not needed for the L x rays because we stabilized on a γ ray in the immediate region of the L x rays. The corrections to the energies of the K x rays are estimated to be about 0.5 to 1.0 keV.

ANALYSIS

The summary of our experimental information is given in Tables II–VI. These tables include the results of the theoretical calculations which will be described. It was possible to determine the energies of 11 K x rays of muonic atoms of Th^{232} and 10 K x rays of muonic atoms of U^{238}. We selected an x ray whose energy was determined with good precision as a reference line, and determined the difference in energy between it and each of the other x rays of the spectrum. Our analysis involved the matching of these energy differences with differencies calculated from a model and the matching of the absolute energy of the reference line to the calculated energy. The differences provided us with experimentally determined quantities with a slightly smaller statistical errors than the absolute values of the energies of the x rays. More important, systematic errors from uncertainties caused by nonlinearity in the analyzer and baseline shifts were limited to the determination of the energy of the reference line.

The calculation of the expected spectrum proceeded from an adaptation of the treatment by Wilets[1] and by Jacobsohn.[2] The electrostatic interaction was split into two parts; the monopole and quadrupole part. The matrix elements of the quadrupole interaction were

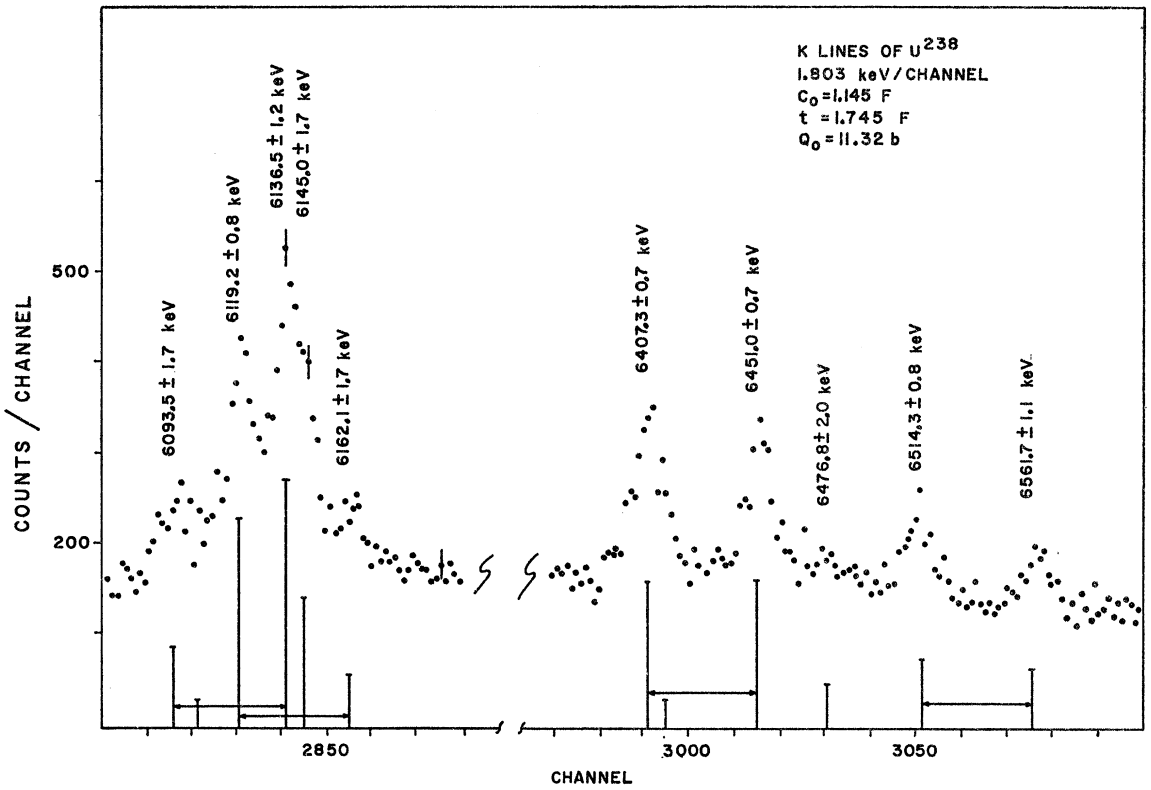

FIG. 3. Spectrum of K x rays (of muonic atoms) of U^{238}.

calculated in a basis system consisting of a linear combination of products of the nuclear wave function and the wave function of the muon. The latter was obtained by the solution of the Dirac equation for a hydrogenlike muonic atom with a potential given by the monopole term of the electrostatic interaction averaged over the nuclear ground state. The nuclear wave function must be obtained from an appropriate nuclear model. We selected wave functions representing pure rotational nuclei for the two nuclei studied in this experiment.

The density of electrical charge in the nucleus is introduced when the monopole term is averaged over the nuclear ground state. We assumed for the charge distribution the modified Fermi distribution:

$$\rho(r,\theta)=\rho_0[1+\exp\{[r(1+\beta P_2(\cos\theta))-c]4.4/t\}]^{-1}, \tag{1}$$

where ρ_0 is approximately the density at the center of the nucleus, β is a measure of the deformation, c is the "half-radius", i.e., the value of the radius at $P_2(\cos)=0$ for which the density has decreased to one-half of ρ_0; t is the surface thickness and is the interval in which the density falls from 90% of ρ_0 to 10% of ρ_0. It is customary to introduce a parameter c_0 related to c by

$$c=c_0A^{1/3}. \tag{2}$$

The monopole term of the interaction

$$H'=(-e^2)\sum_{p=1}^{z}|\,\mathbf{r}p-\mathbf{r}_\mu\,|^{-1}, \tag{3}$$

when averaged over the wave function of the nuclear ground state, is equivalent to the spherical average of the potential of the charge-density equation (1). The position vectors of the proton and the muon are $\mathbf{r}_p$ and $\mathbf{r}_\mu$, respectively. This potential as seen by the muon is

$$V(r_\mu)=(-e^2)\rho(0)2\pi\left[\int_0^{r_\mu}\frac{r^2}{r_\mu}v(r)\,dr+\int_{r_\mu}^{\infty}rv(r)\,dr\right], \tag{4}$$

$$v(r)=\int_{-1}^{1}f(r,y)\,dy=2f_0, \tag{5}$$

where r_μ is the magnitude of the radius vector to the muon, r is the magnitude of the radius vector to an element of charge in the nucleus, and $f(r,y)$ is defined in the following. We rewrite Eq. (1) as

$$\rho(r,\theta)=\rho(0)f(r,\cos\theta), \tag{6}$$

$$f(r,\cos\theta)=\sum_l\left(\tfrac{1}{2}(2l+1)\int_{-1}^{1}f(r,y)\,P_l(y)\,dy\right)P_l(\cos\theta) \tag{7}$$

$$=\sum_l f_l(r)\,P_l(\cos\theta); \tag{8}$$

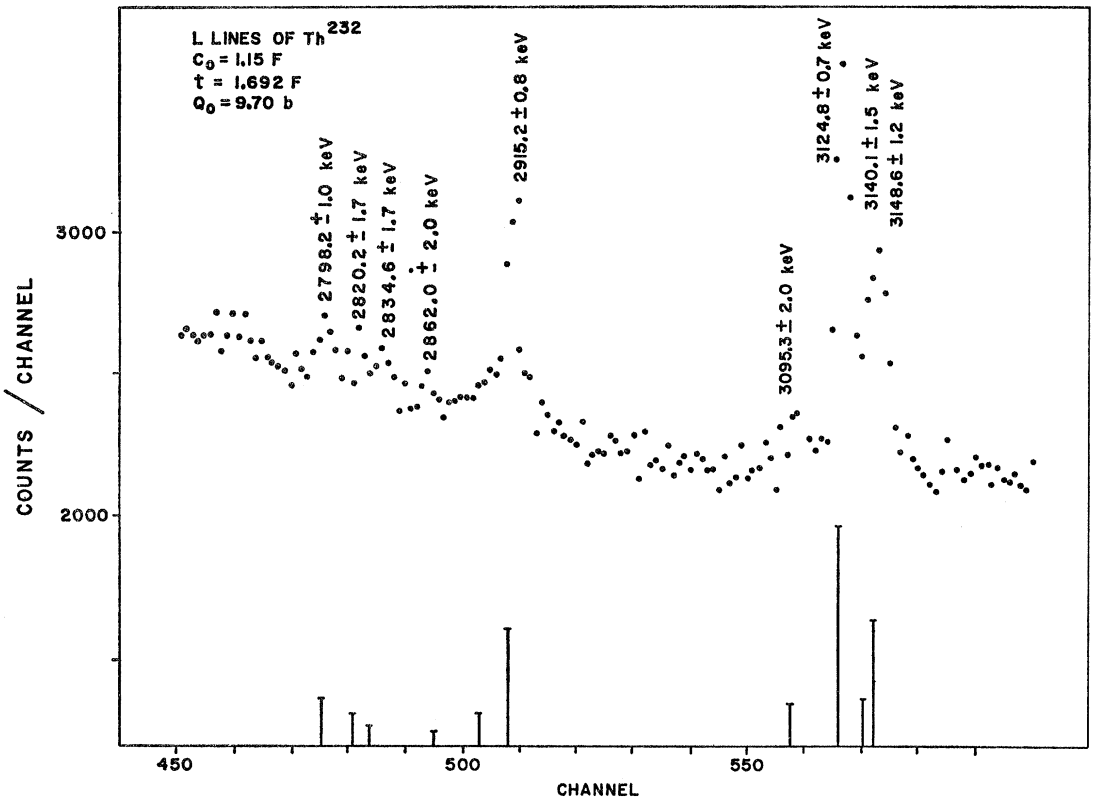

FIG. 4. Spectrum of L x rays (of muonic atoms) of Th^{232}.

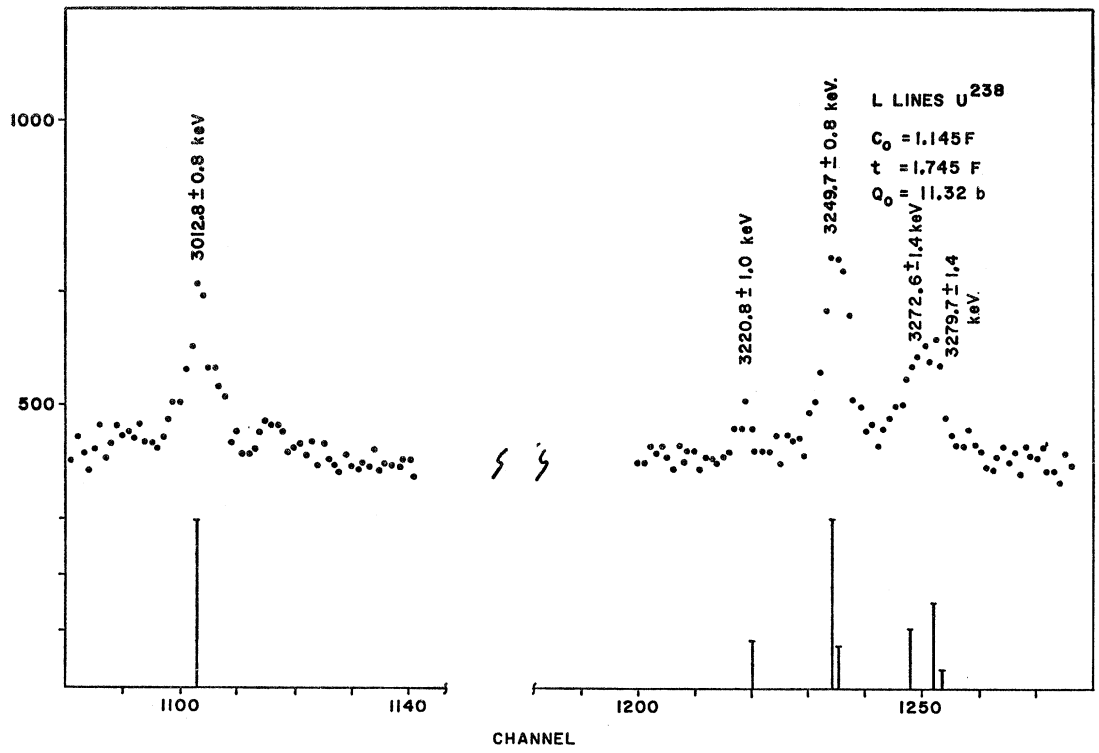

FIG. 5. Spectrum of L x rays (of muonic atoms) of U^{238}.

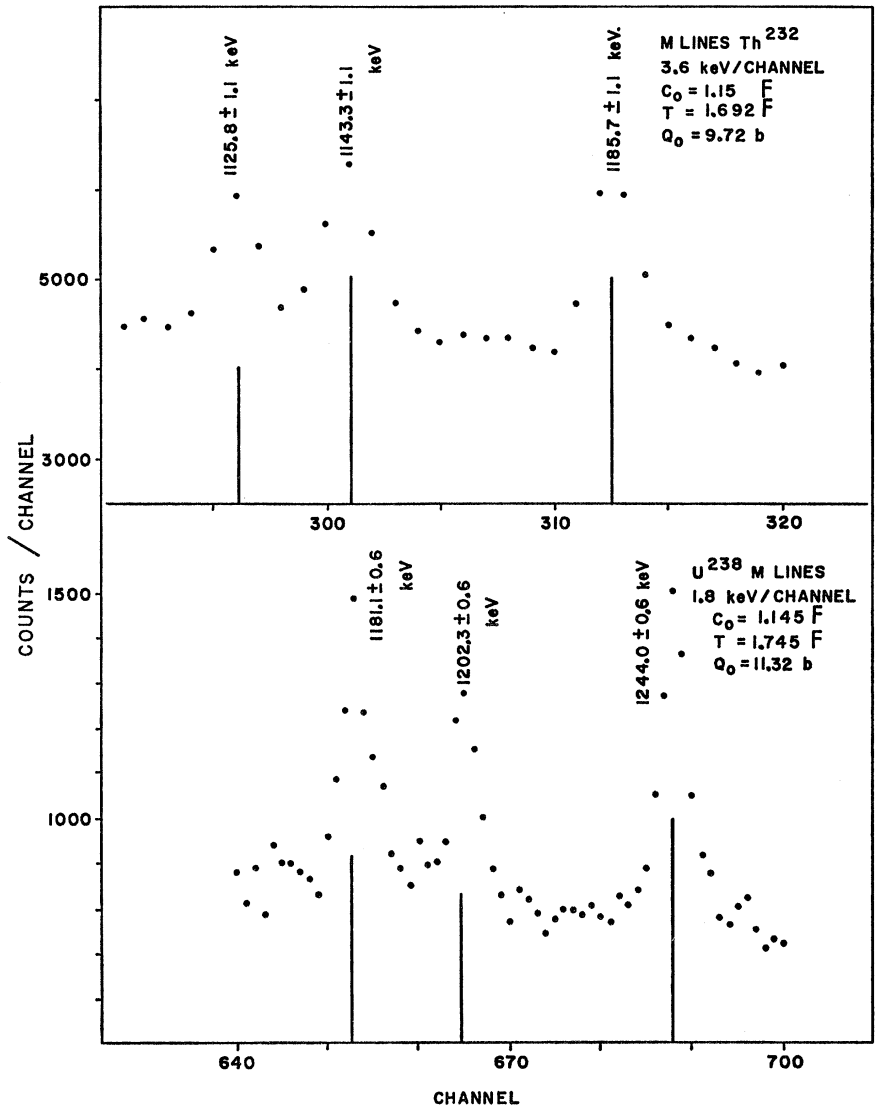

FIG. 6 (a) Spectrum of M x rays (of muonic atoms) of Th^{232}. (b) Spectrum of M x rays (of muonic atoms) of U^{238}.

$\rho(0)$ is obtained by a normalization to the total charge:

$$\rho(0)=\left(Z \Big/ 2\pi\int_0^\infty \int_{-1}^{1} f(r,y)r^2 dr dy\right). \quad (9)$$

We adjusted the potential of Eq. (4) to include a term to allow for the increase in binding caused by the vacuum polarization. We start with the approximate expression for the potential caused by the vacuum polarization[6]

$$V(r)=(2\alpha/3\pi)[V_L(r)-\tfrac{5}{6}V(r)]. \quad (10)$$

$V(r)$ is the electrostatic potential, α is the fine structure constant, and $V_L(r)$ is given by

$$V_L(r_\mu)=e^2\iiint \ln[C\,|\,\mathbf{r}_\mu-\mathbf{r}\,|\,/\lambda\!\!\!^{-}_e]\frac{\rho(r)d^3r}{|\,\mathbf{r}_\mu-\mathbf{r}\,|}, \quad (11)$$

$\rho(r)$ is the charge density, $\lambda\!\!\!^{-}_e$ is the reduced compton wavelength for the electron, and $C=1.781$. With some manipulation, we arrived at the following potential in which x is the displacement, in units of $\hbar/mc$:

$$\phi(x_\mu)=v(x_\mu)\{1-(2\alpha/3\pi)[\tfrac{5}{6}+\ln(x_\mu^2+\epsilon^2)^{1/2}b]\}. \quad (12)$$

$v(x_\mu)$ is the potential derived from the monopole part of the electrostatic interaction. $b=m/[m_e(1.781)]$; m_e is the mass of the electron, m is the reduced muon mass, and ϵ is a small quantity introduced to avoid the singularity in the logarithm term at the origin. We took $\epsilon=0.125$ muon Compton wavelengths. The introduction of ϵ involves neglecting a small term in the potential of the vacuum polarization.[7]

The matrix elements of the quadrupole interaction

[6] David L. Hill and Kenneth W. Ford, Phys. Rev. 94, 1617 (1954).

[7] We have been informed by J. McKinley that this procedure neglects a contribution of about 1.5 keV to the p levels.

TABLE II. K x rays of muonic atoms of Th^{232}.

Energies of observed x rays (keV)	Calculated energies[a] (keV)	Intensities of observed x rays relative to 6350.5	Calculated intensities[a] relative to transition of 6350.5 keV
6021.5±1.3	6019.4	0.50±0.13	0.46
6050.2±0.8	6050.8	1.8±0.4	1.5
6067.4±1.0	6067.8	2.5±0.6	1.9
6077.2±1.3	6074.3	1.0±0.3	0.9
6098.5±1.3	6099.2	0.40±0.12	0.3
6272.2±2.6	6272.3	0.16±0.08	0.13
6302.2±0.9	6302.3	0.93±0.20	0.82
6313.4±3.3	6314.3	0.22±0.12	0.16
6350.5±0.7	6350.7	standard i.e., 1.0	1.00
6380.4±1.2	6378.9	0.38±0.10	0.33
6403.2±0.9	6403.8	0.65±0.20	0.55

[a] $c_0=1.15$ F, $t=1.692$ F, $Q_0=9.70$ b.

are calculated between states

$$|IJFM_F\rangle = \sum_{M_I,M_J} (IJM_IM_J \mid FM_F)\,|IM_I\rangle\,|JM_J\rangle, \quad (13)$$

where the $(IJM_IM_J \mid FM_F)$ are the vector addition coefficients $|IM_I\rangle$ are nuclear wave functions and $|JM_J\rangle$ are muonic wave functions obtained from solutions of the Dirac equation.

The matrix elements are given by

$$(IJFM_F \mid H_Q \mid I'J'FM_F) = (-1)^{I'+J-F}[20\Pi(2I'+1)(2J+1)]^{1/2}(J \,||\, Y_2 \,||\, J') \times W(IJI'J';F2)(2I'OK \mid IK)\alpha(JJ'), \quad (14)$$

where we have specialized to deformed nuclei. $W(IJI'J';F2)$ is the Racah coefficient. The reduced

TABLE III. K x rays of muonic atoms of U^{238}.

Energies of observed x rays (keV)	Calculated energies[a] (keV)	Intensities of observed x rays relative to transition of 6451.0 keV	Calculated intensities[a] relative to transition of 6451.0 keV
6093.5±1.7	6092.6	0.56±0.10	0.49
6119.2±0.8	6119.1	1.59±0.18	1.33
6136.5±1.2	6137.3	1.68±0.26	1.63
6145.0±1.7	6145.6	1.17±0.22	0.82
6162.1±1.7	6163.8	0.30±0.10	0.3
6407.3±0.7	6406.8	1.05±0.12	0.99
6451.0±0.7	6451.5	standard	standard
6476.8±2.0	6479.1	0.18±0.05	0.27
6514.3±0.8	6515.7	0.58±0.08	0.46
6561.7±1.1	6560.4	0.38±0.07	0.24

[a] $c_0=1.145$ F, $t=1.745$ F, $Q_0=11.32$ b.

TABLE IV. *L* x rays.

Muonic atoms of Th^{232} Experimental (keV)	Muonic atoms of Th^{232} Calculated[a] (keV)	Muonic atoms of U^{238} Experimental (keV)	Muonic atoms of U^{238} Calculated[b] (keV)	Weighted average for doublets
2798.2±1.0	2795.3	3012.8±0.8	3011.7	
2820.2±1.7	2820.7	3220.8±1.0	3221.6	
2834.6±1.7	2830.3	3249.7±0.8	3248.1 3251.7	3248.6
2862.0±2.0	2865.3			
2903.1±3.0	2897.3	3272.6±1.4	3272.8	
2915.2±0.8	2914.5	3279.7±1.4	3278.2 3281.0	3278.6
3095.3±2.0	3093.8			
3124.8±0.7	3125.2			
3140.1±1.5	3142.6			
3148.6±1.2	3149.1			

[a] $c_0=1.15$ F, $t=1.692$ F, $Q_0=9.70$ b.

[b] $c_0=1.145$ F, $t=1.745$ F, $Q_0=11.32$ b.

TABLE V. *M* x rays of muonic atoms.

Energies (keV) Experimental	Energies (keV) Calculated	Th^{232} Intensities Relative to transition 1125.8 keV Experimental	Th^{232} Intensities Relative to transition 1125.8 keV Calculated	CERN Experimental data energies (keV)
1125.8±1.1	1127.01[a]	standard	standard[a]	1129.3±1.9
1143.3±1.1	1144.2	1.3±0.2	1.3	1145.3±1.9
1185.7±1.1	1185.9	1.2±0.2	1.6	1187.1±2.0
		U^{238} Relative to 1181.1		
1181.1±0.6	1181.1[b]	standard	standard[b]	1182.9±1.5
1202.3±0.6	1202.3	0.78±0.11	0.81	1202.1±1.5
1244.0±0.6	1244.3	1.3±0.1	1.24	1245.2±1.6

[a] $c_0=1.15$ F, $t=1.692$ F, $Q_0=9.72$ b.

[b] $c_0=1.145$ F, $t=1.745$ F, $Q_0=11.32$ b.

TABLE VI. *N* x rays of muonic atoms.

Experimental energies (keV)	Calculated Energies: Finite nucleus vacuum polarization (keV)	Finite nucleus no vacuum polarization (keV)	Point nucleus no vacuum polarization (keV)	Intensities Expt.	Intensities Calc.	CERN experimental data energies (keV)
			Th^{232}			
520.5±0.3	520.79	518.18	518.25	1.4±0.1	1.3	526.5±1.3
530.3±0.3	530.18	527.40	527.42			
			U^{238}			
544.6±0.5	544.52	541.75	541.75	1.2±0.1	1.3	549.6±1.3
554.5±0.5	554.78	551.83	551.83			

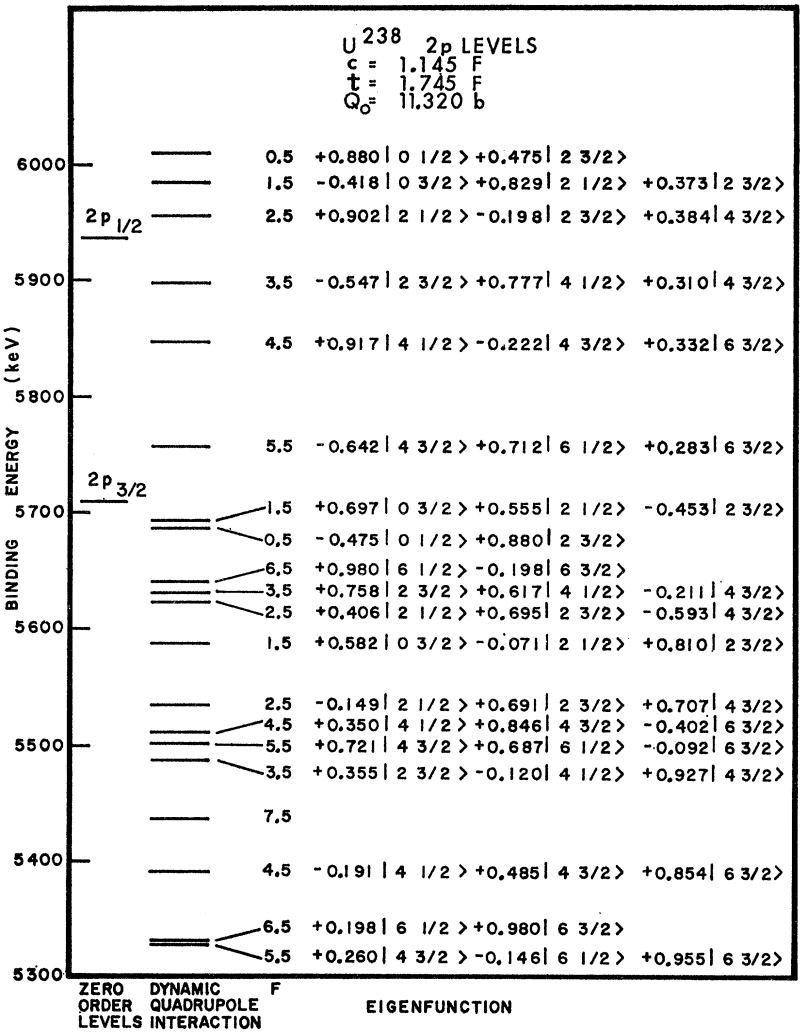

FIG. 7. Multiplet structure of $2p$ levels of muonic atoms of U^{238} with dynamic quadrupole interaction included. The levels are labeled by F, the quantum number for total angular momentum. The eigenfunctions are given as linear combinations of basis functions for which the angular momentum of the muon J, the spin of the nucleus, I, the total angular momentum F, and the projection of F, M_F are diagonal. Note the coefficients are independent of M_F. These basis functions are in turn linear combinations of products of hydrogenlike wave functions of muonic atoms and nuclear wave functions.

matrix element $(J \,||\, Y_2 \,||\, J')$ is defined by

$$(2J'qm_{J'} \mid Jm_J)(J \,||\, Y_2 \,||\, J') = (Jm_J \mid Y_2{}^q \mid J'm_{J'}). \tag{15}$$

$\alpha(JJ')$ contains the dependence on the intrinsic quadrupole moment and the penetrability factor:

$$\alpha(JJ') = \frac{-e^2}{5} \int_0^\infty R_{\epsilon J} R_{\epsilon J'} q(r_\mu) r_\mu{}^2 dr_\mu; \tag{16}$$

$R_{\epsilon J}$ is the radial part of the wave function of the muonic atom in a state with energy eigenvalue ϵ and total angular momentum J, and

$$q(r_\mu) = \int_0^\pi \int_0^{2\pi} \int_0^{r_\mu} \rho(r,\theta) P_2(\theta) \frac{r^2}{r_\mu{}^3} d^3r + \int_0^\pi \int_0^{2\pi} \int_{r_\mu}^\infty \rho(r,\theta) P_2(\theta) \frac{r_\mu{}^2}{r^3} d^3r. \tag{17}$$

In terms of the reduced matrix used by the group at CERN,[8,9] our α is given by

$$\langle j \,||f||\, j' \rangle = (10/Q_0 e^2)\alpha(JJ') = (6.945/Q_0)\alpha(jj') \times 10^{-5}\,\mathrm{F}^{-3}. \tag{18}$$

The matrix for the quadrupole interaction was then diagonalized to get the energy eigenvalues. This was done for the muon in the $2p$ orbit and for the muon in the $3d$ orbit. Figures 7 and 8 show the final multiplet structure and the corresponding eigenfunctions for the $2p$ and $3d$ levels of U^{238}.

The intensities of the x ray can be calculated from the standard electric dipole transition probabilities for transitions between the $3d$ states and the $2p$ states and transitions between the $2p$ states and the $1s$ states. For this calculation, we assumed that the $4f$ states are populated statistically and that there are no contributions from states $l<(n-1)$. The intensities of the K

[8] S. A. DeWit, G. Backenstoss, C. Daum, J. C. Sens, and H. L. Acker, Nucl. Phys. **87**, 657 (1967).
[9] H. L. Acker, Nucl. Phys. **87**, 153 (1966).

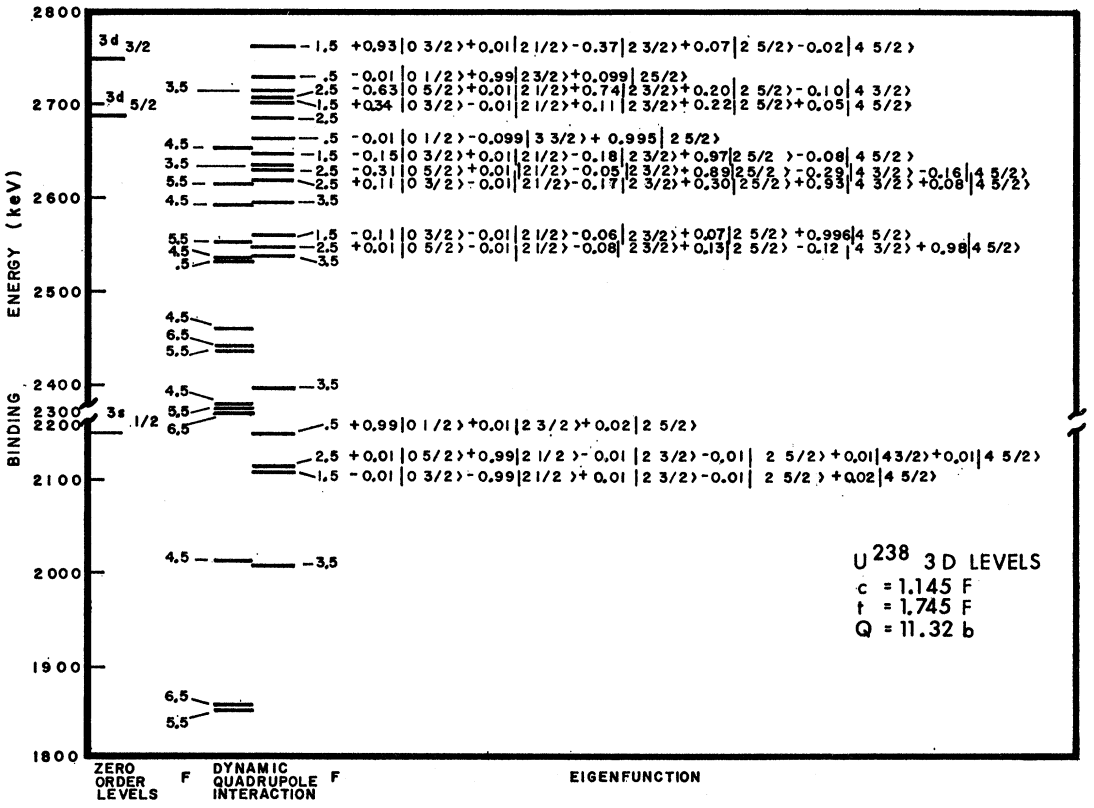

FIG. 8. Multiplet structure of $3d$ levels of muonic atoms of U^{238}.

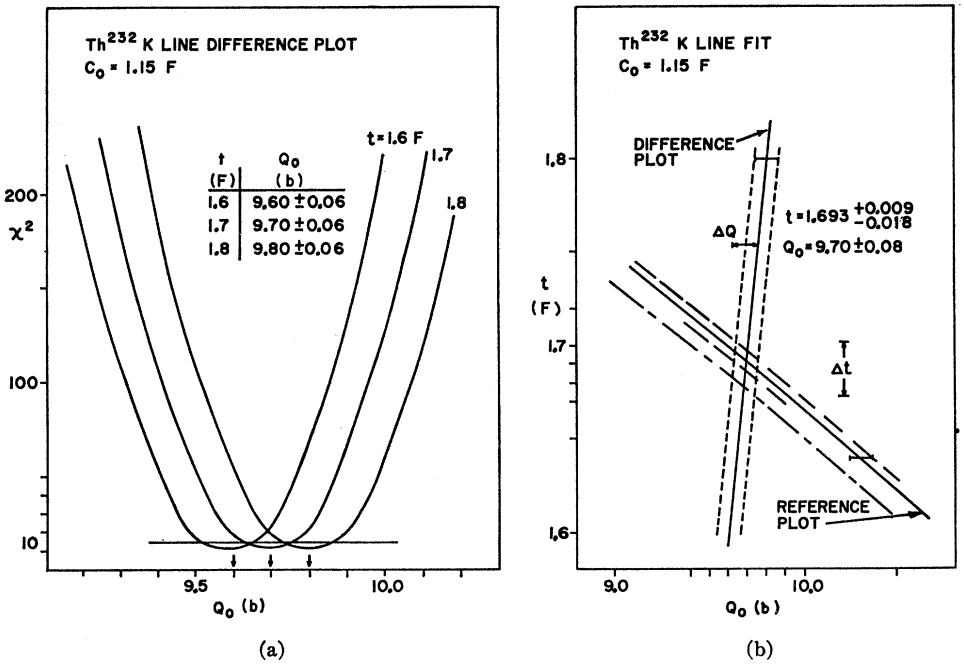

FIG. 9(a). Typical plots of χ^2 versus Q_0, intrinsic quadrupole moment, for a particular value of the half-radius parameter c_0, and selected values of the surface thickness t. The values of Q_0 which minimize each curve are shown. (b) Typical plots of Q_0 and t for which the values of χ^2 in (a) are a minimum. We also show plots of Q_0 and t which yield the energy of the reference transition within the experimental error. Note the asymmetric errors in the reference line; these take into account possible baseline shifts.

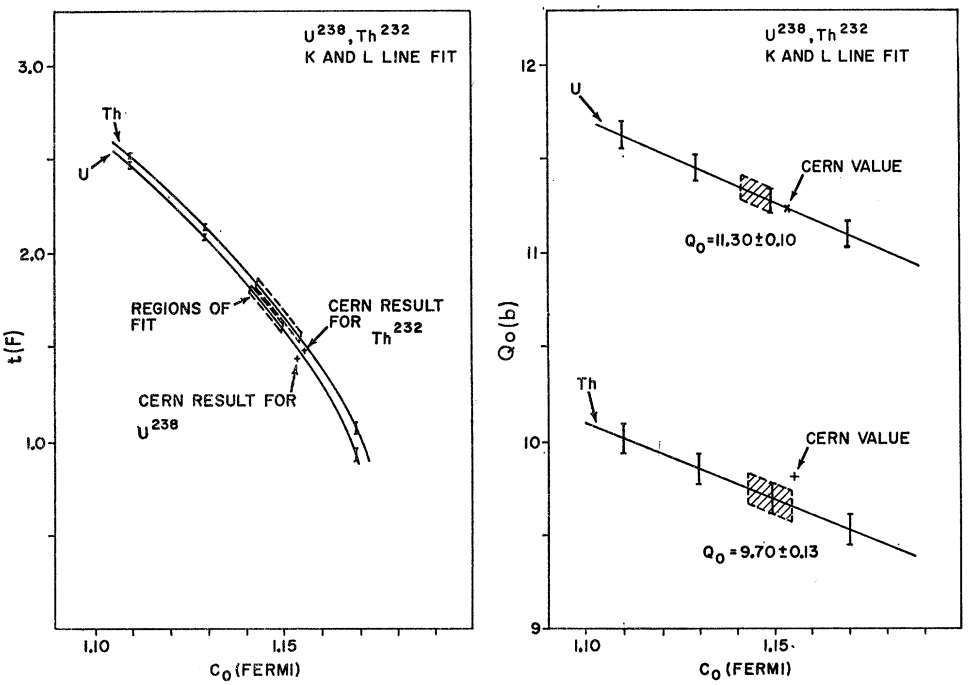

(a) (b)

FIG. 10(a). Locus of points in (c_0, t) space which fit the K lines. Bounded regions indicate values of parameters which fit L lines also. Vertical bars are precision measures determined from extent of area of acceptable values of Q_0 and t for values of c_0 as in Fig. 9(b). (b) Corresponding plot in (c_0, Q_0) space. Vertical bars have corresponding significance.

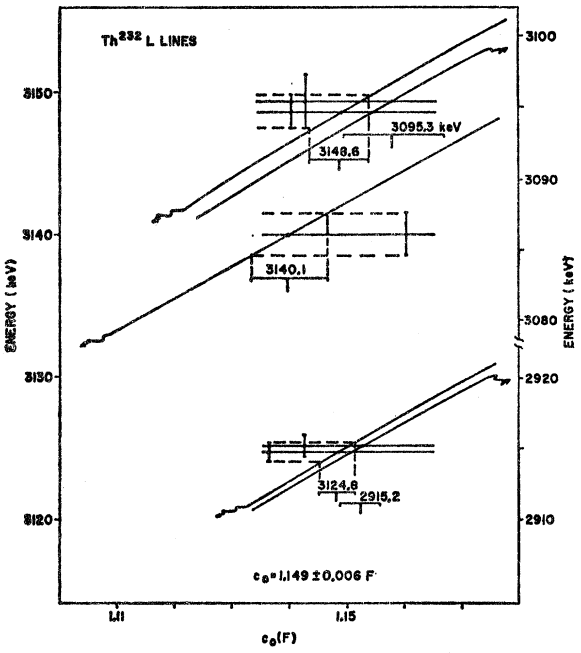

FIG. 11. Typical plot of energies of L x rays calculated for values of c_0, t, and Q_0 which reproduce the energies of the K transitions. Arrows on L transitions indicate which vertical scale applies. Horizontal lines represent experimental results with errors.

transitions from states of energy eigenvalue λ_2 and total angular quantum number F_2 to states of energy λ_i, are given by

$$I(\lambda_2 F_2 \rightarrow \lambda_i) = \frac{P(\lambda_2 F_2)\,(\lambda_2-\lambda_i)^3 \sum_J |\,(F_2 I_i J \mid F_2 \lambda_2)\,|^2 [R(JJ')]^2}{\sum_{\lambda_i} (\lambda_2-\lambda_i)^3 \sum_J |\,(F_2 I_i J \mid F_2 \lambda_2)\,|^2 [R(JJ')]^2}, \tag{19}$$

where I_i and J are nuclear muonic angular momentum quantum numbers which combine to give F_2. $P(\lambda_2 F_2)$ is the population of the initial state characterized by λ_2, F_2. $(F_2 I_i J \mid F_2 \lambda_2)$ are the coefficients of the linear combination of basis functions described above which yield the basis in which the quadrupole interaction is diagonal. $R(JJ')$ are the radial integrals for the dipole transitions of the muonic atom and are given by

$$R(JJ') = \int_0^\infty R_{\epsilon J} r^3 R_{\epsilon' J'} dr. \tag{20}$$

$R_{\epsilon J}$ is the radial part of the solution of the Dirac equation where the potential is calculated for a nucleus of finite extent. Apart from details of the correction for the vacuum polarization, our analysis has the same physical content as that of CERN.[8,9] In a later part of

TABLE VII. Parameter sets which fit the data.

Regions of fit: U^{238}			Regions of fit: Th^{232}		
c_0 (F)	t (F)	Q_0 (b)	c_0 (F)	t (F)	Q_0 (F)
		This experiment			
1.150	$1.615\pm^{0.009}_{0.015}$[a]	11.27±0.07	1.155	$1.56\pm^{0.01}_{0.02}$	9.66±0.08
1.146	$1.72\pm^{0.01}_{0.02}$	11.30±0.07	1.150	$1.69\pm^{0.009}_{0.018}$[a]	9.70±0.08
1.145	$1.745\pm^{0.009}_{0.015}$[a]	11.32±0.07	1.145	$1.81\pm^{0.01}_{0.02}$	9.73±0.08
1.142	$1.86\pm^{0.01}_{0.02}$	11.34±0.07	1.143	$1.86\pm^{0.01}_{0.02}$	9.75±0.08
		CERN[b]			
1.154	1.46	11.25	1.155	1.49	9.8

[a] These values were determined from Q_0-t plot. All other values are extrapolated values from the graphs of c_0 versus t, and Q_0 versus t.

[b] Reference 8.

this paper we compare the results of an actual calculation with theirs.

We start the analysis of the data with a guess of the values for c_0, t, and Q_0. In Table I the values of the physical constants used in this calculation are presented. It should be observed that three nuclear levels of Th^{232} and four nuclear levels of U^{238} were used in the calculation. From the experimental data we calculated the energy of a reference x-ray transition and the difference in energy of 10 other transitions in Th^{232} from the reference line and the difference in energy of 9 transitions from the reference line of U^{238}. The χ^2 for these differences was calculated with an assumed value of c_0, t, and several values of Q_0. A family of curves χ^2 versus Q_0 were obtained for a fixed c_0 and different t. A typical family of curves is shown in Fig. 9(a), each member of the family goes through a minimum χ^2 which then gave us a Q_0 corresponding to the t of the curve and c_0 of the family.

The minimum values of the $\chi^2=(\chi^2)_{\min}$ thus obtained, were typically about 10 for Th^{232} and about 11 for U^{238}. We selected the statistical error in Q_0 to correspond to a spread $\Delta Q_0'$ about $(\chi^2)_{\min}$ which gives a probability of 75% that the true χ^2 lies in this range.

The set of $(Q_0+\Delta Q_0', t)$ derived from this family are graphed in Fig. 9(b). This is a plot of acceptable pairs of Q_0 and t for a particular c_0 which will match the experimental differences of the K x-ray data. It is to be noted that the reference line is done separately. In Fig. 9(b), we also show the locus of points in (Q_0, t) space which fit the energy of the reference line in Th^{232} for a given c_0. The region of intersection of the two bands gives us an area $(Q_0\pm\Delta Q_0,\ t\pm\Delta t)$ which will yield the K x-ray data. The shape and extent of the area is indicative of the statistical correlation of Q_0 and t. All pairs of Q_0 and t falling within this area will lead to an acceptable set of results. A qualitative measure of the area is given by the maximum extension of Q_0 and t. It is the maximum extensions on either side of the fit that we quote as precision measures ΔQ_0 and Δt. The baseline shift of the K lines has been taken into account by introducing an asymmetric error band in the (Q_0, t) reference plot, as shown in Fig. 9(b). We did not correct the energies of the K lines but increased the errors only. The analysis is repeated for different values of c_0 with suitable changes in t but very slight changes in Q_0. The result, presented in Figs. 10(a) and 10(b), show a volume in Q_0, t, c_0 space which encloses our sets of values of the three parameters which give acceptable fits. Figure 10(a) is a projection of this volume in the c_0, t plane. The points with error bars represent actual calculations; the rest of the curve is an extrapolation. Figure 10(b) is a projection on the Q_0, c_0 plane where the bars on the curve are values obtained from actual calculations while the rest of the curve is extrapolated.

The data corresponding to the L transitions are used to narrow the range of acceptable values of the parameters. The energies of the L transitions and intensities were calculated for the sets of parameters which fit the K x-ray data. The complexity of the L spectrum forced us to select a few prominent transitions. The energies corresponding to these transitions are plotted as a function of c_0 in Fig. 11 for the appropriate t and Q_0 which fit the K x-ray data. It is seen from the figure that the experimentally determined energies of the L transitions narrows the region of acceptable values of the parameters.

The results of these measurements are given in

TABLE VIII. Radial matrix elements $\langle nj \mid f(r) \mid nj' \rangle$.

n	j	j'	$\langle j \mid f \mid j' \rangle$ (F^{-3}) (this expt) Values$\times 10^{-4}$	CERN[a] ($\times 10^{-4}$)	$\langle j \mid f \mid j' \rangle$ (F^{-3}) (this expt) Values$\times 10^{-4}$	CERN[a] ($\times 10^{-4}$)
2	$\frac{3}{2}$	$\frac{1}{2}$	5.795–5.865[b]	5.849	5.751–5.818[c]	5.782
2	$\frac{3}{2}$	$\frac{3}{2}$	5.860–5.930	5.912	5.805–5.872	5.835
3	$\frac{3}{2}$	$\frac{5}{2}$	1.313–1.319	1.303	1.238–1.243	1.226
3	$\frac{3}{2}$	$\frac{5}{2}$	1.149–1.153	1.139	1.084–1.088	1.074
3	$\frac{5}{2}$	$\frac{5}{2}$	1.131–1.135	1.122	1.067–1.071	1.058
3	$\frac{1}{2}$	$\frac{3}{2}$	0.338		0.314	
3	$\frac{1}{2}$	$\frac{5}{2}$	0.266		0.247	

[a] Reference 8.

[b] These values include: $c=1.142$–1.150 F; $t=1.870$–1.60 F; $Q=11.41$–11.20 b.

[c] These values include: $c=1.143$–1.155 F; $t=1.870$–1.540 F; $Q=9.83$–9.580 b.

Table VII. The quoted ranges in Q_0 and t are the maximum extension of the areas in the Q_0-t plots for each c_0. Note that the spread quoted for c_0 derives mainly from the experimental errors of the L lines. We consider these errors as defining a band of acceptable values of c_0. Within this band, one can determine values of t and Q_0 from Figs. 10(a) and 10(b), and assign precision measures to t and Q_0 for particular values of c_0.

TABLE IX. K transitions in muonic atoms of U^{238}. Comparison of calculations of this paper with those of group at CERN.[a] Parameters $c_0=1.154$ F, $t=1.46$ F, $Q_0=11.25$ b

This paper Energy (keV)	Relative intensity		CERN Energy (keV)	Relative intensity
6096.6	0.49		6096.9	0.47
6123.1	1.26		6123.5	1.30
6141.3	1.51		6141.6	1.62
6149.7	0.74		6149.9	0.82
6411.6	0.96		6410.6	1.01
6456.3	1.00		6455.3	1.00
6520.7	0.46		6519.5	0.46
6565.4	0.24		6564.2	0.24
		L transitions		
3014.9	3.80		3013.2	3.67
3225.7	0.98		3223.0	0.92
3252.1	4.17		3249.6	4.03
3276.9	1.00		3273.9	1.00
3282.0	1.89		3279.5	1.79
Energy above ground state		Unperturbed levels		
6214.1		$2P_{1/2}$	6213.6	
6442.9		$2P_{3/2}$	6442.4	
9402.8		$3D_{3/2}$	9400.3	
9468.8		$3D_{5/2}$	9466.1	
10 637.9		$4F_{5/2}$	10 634.1	
10 652.5		$4F_{7/2}$	10 648.7	

[a] Reference 8.

CONCLUSIONS

It can be seen from Tables II and III that the calculated values of the K x rays of Th^{232} and U^{238} agree with the measured values within the experimental errors. An analysis of the discrepancies yield a χ^2 of 10.2 for Th^{232}, and 8.6 for U^{238}. We selected values for c_0, t, and Q_0 from the heart of the region of acceptable values to calculate the muonic x-ray spectra summarized in Tables II–VI.

The agreement between the calculated values and the measured values of the L x rays of Th^{232} is not satisfactory. In the L spectrum of Th^{232} there are unexplained discrepancies of two or more standard deviations for some transitions.

Our technique for the determination of the energies and assignment of errors of observed transitions is suspect for the weak transitions, particularly when near in energy to more intense transitions. We have accepted the results of this computational procedure for all of the experimental data, but admit that we have not evaluated the background influences quantitatively.

The calculated values of the energies and intensities of the M and N x rays agree with the experimental values.

The correction for vacuum polarization for the calculation of the energies of the N lines is about 3 keV, and is absolutely essential to obtain agreement with the experiment. We note from Table VI that calculations of the energies of the N transitions are insensitive to the finite extent of the nucleus. The shifts in the 5 g and 4 f levels due to electron shells[10] can be estimated to be about 0.2 and 0.1 keV, respectively, so that the N-line transition energy increases by about 0.1 keV. This

[10] R. C. Barret, S. J. Brodsky, G. W. Erickson, and M. H. Goldhaber, Phys. Rev. **166**, 1589 (1968).

TABLE X. Experimental measurements of Q_0 (in barns).

	This experiment	CERN[a]	Coulomb excitation[b]	Coulomb excitation[c]
Th^{232}	9.58–9.83	9.8	10.8	9.25±0.23
U^{238}	11.20–11.41	11.25	11.5	9.98±0.28

[a] Muonic x rays (Reference 8).
[b] D. Y. Rester, M. S. Moore, F. E. Durham, C. M. Class, Nucl. Phys. **22**, 14 (1961).
[c] R. E. Bill, S. Bjornholm, J. C. Severieus, Kgl. Danske Videnskab Selskab, Mat.-Fys. Medd. **32**, No. 12 (1960).

correction was not taken into account in the N-line calculation. The values of M and N lines are in agreement with those reported by DeWit *et al.*[8]

Nuclear polarization effects were neglected. In the case of $1s$ and $2p$ levels, they are expected to produce a shift of about -1.2 keV,[11] and therefore have small effect on the K-transition energy. The $3d$ shift is negligible, about 0.1 keV, so that the L lines may be 1 keV higher than given by the present calculation. With the present accuracy, a 1-keV change in L lines would not affect the final values of c_0, t, and Q_0 appreciably. It is possible that in the presence of a muon, the nuclear excited state, $I=2^+$, would be increased in energy by 1 keV.[11] By measuring the difference between two lines originating from a common $n=2$ state and terminating on $n=1$ levels corresponding to the nucleus either in the ground state or excited state, one can measure the energy difference of the system muon-plus-nucleus in the ground state and muon-plus-nucleus excited. This yields the same information as a measurement of the nuclear γ ray with the muon in the $1s$ state. Our results give 48.3±1.0 and 108.2±3.0 keV for the 2^+-0^+ and 4^+-2^+ difference, respectively, in the Th^{232} and 43.7± 1 keV for the 2^+-0^+ difference in U^{238}. Upon comparing the above results to the measurements of the nuclear γ rays,[12,13] 49.75±0.25, 112.7±1.0 for the Th^{232} and 44.7±0.2 for U^{238}, one concludes that there is no evidence for a shift due to nuclear polarization predicted by Pieper and Greiner.[11]

The comparison of our results of c_0, t, and Q_0 with those of CERN[8] is given in Table VII. A set of radial matrix elements $\langle j | f(r) | j' \rangle$ for an acceptable set of parameters is given in Table VIII. The expression for the radial matrix elements is related to the reduction of the quadrupole interaction due to finite size effect. As expected, the magnitude decreases with n, the principal quantum number. We have calculated the energies of the most intense K and L transitions for muonic U^{238} for the parameters selected by the group at CERN.[8,9] The results of our calculation are compared to the CERN calculations in Table IX. The energies of the K transitions compare very well. We attribute the differences to slight differences in c_0. We converted the value of c given to three significant figures by the group at CERN to c_0 for our calculation. The differences in the energies of the L transitions were attribute to different methods for the calculation of the vacuum polarization.

The results of measurements of Q_0 by different groups is presented in Table X. We must emphasize that our results depend on the model we use. The range of c_0, t, and Q_0 have meaning only for the modified Fermi distribution we used.

ACKNOWLEDGMENTS

We are greatly indebted to D. G. Ravenhall of the University of Illinois for many illuminating discussions. Our computational procedures were developed by following important suggestions from Professor Ravenhall.

We are grateful to H. Mann and his group at the Argonne National Laboratory for providing the supberb Ge(Li) detectors used throughout the experiment. We acknowledge gratefully that much of the detailed computational work was done by J. Gray and G. Kessler at the State University of New York at Binghamton.

[11] W. Pieper, and W. Greiner, Nucl. Phys. **A109**, 539 (1968); Phys. Letters **24B**, 377 (1967).
[12] F. S. Stephens, Jr., R. M. Diamond, and I. Pearlman, Phys. Rev. Letters **3**, 435 (1959) with addendum by K. Alder and A. Winther, in *Coulomb Excitation* (Academic Press Inc., New York, 1966).
[13] J. O. Newton, Nucl. Phys. **3**, 345 (1957).